

# Covalent grafting of phenylphosphonate groups onto layered silica derived from *in situ*-leached chrysotile fibers

Fernando Wypych,<sup>\*a</sup> Wido H. Schreiner,<sup>b</sup> Ney Mattoso,<sup>b</sup> Dante H. Mosca,<sup>b</sup> Rafael Marangoni<sup>a</sup> and Carlos A. da S. Bento<sup>c</sup>

<sup>a</sup>Centro de Pesquisas em Química Aplicada (CEPESQ), Departamento de Química, Universidade Federal do Paraná (UFPR), CP 19081, 81531-990 Curitiba PR, Brazil.  
E-mail: wypych@quimica.ufpr.br

<sup>b</sup>Departamento de Física, Universidade Federal do Paraná (UFPR), CP 19081, 81531-990 Curitiba PR, Brazil

<sup>c</sup>Laboratório de Microscopia Eletrônica de Varredura, Instituto de Química, Universidade de São Paulo (USP/São Carlos), 13560-970 São Carlos SP, Brazil

Received 22nd November 2002, Accepted 12th December 2002

First published as an Advance Article on the web 7th January 2003

The reaction of natural chrysotile fibers with phenylphosphonic acid leads to a new grafted material. The layered material, with an interplanar basal distance of 15.2 Å, was characterized by powder X-ray diffraction, thermal analysis, X-ray photoelectron spectroscopy, Fourier transform infrared spectroscopy, transmission electron microscopy and energy dispersive X-ray analysis. The experimental data are consistent with the grafting of phenylphosphonate groups to the surface of the layered silica sheets, obtained by the *in situ* acidic leaching of brucite sheets, from chrysotile.

## 1 Introduction

There are several reports in the literature on grafting reactions involving layered structures.<sup>1–5</sup> The reactions are mainly governed by the covalent bonding of specific reactive molecules to the surface of the matrix, producing layered mineral–organic hybrid compounds. Examples using mineral clays as matrices have been reported,<sup>1,6–9</sup> and the grafting of specific molecules to the hydroxylated side of kaolinite layers has been a topic of considerable interest.<sup>10–17</sup> Matrices with non-reactive layers can also be used. These produce a partial disruption of the structure, but still remain layered and incorporate the grafted species<sup>18</sup> with reaction at the outer surface.<sup>9</sup>

Chrysotile is classified in the kaolin 1:1 minerals group.<sup>19</sup> Kaolinite [Al<sub>2</sub>Si<sub>2</sub>O<sub>5</sub>(OH)<sub>4</sub>] is a dioctahedral 1:1 layered aluminosilicate, consisting of octahedral sheets of gibbsite covalently bonded to a tetrahedral sheets of silicate (tridymite), with a regular layered structure.<sup>19</sup> The aluminium atoms are positioned at the octahedral centers and the hydroxyl groups are located at the octahedral vertices.

In contrast to kaolinite, chrysotile displays substitution of aluminium atoms by magnesium, which form a compact layer of brucite.<sup>19</sup> The mismatch of the brucite octahedral sheet with the silica tetrahedral sheet causes the curvature of the layers, which roll into tight tubes, the characteristic chrysotile fibers. The octahedral sheet is situated on the outer convex side. Iron is a common impurity in chrysotile due to extended weathering on the geological timescale.

Chrysotile may be leached with acids or reacted with silanes,<sup>20</sup> resulting in layered hydrated silica or silica functionalized with silane groups, respectively.

## 2 Experimental

A chrysotile sample with fiber lengths of less than 2.0 mm (SAMA7ML) was supplied by SAMA—Mineração de Amianto Ltda, mined in Uruaçu, Goiás, Brazil. The sample preparation included magnetite removal, soaking and washing the chrysotile in distilled water, and drying for 24 h at 100 °C.

Afterwards, 0.2 g ( $7.22 \times 10^{-4}$  mol) of chrysotile were added to 30 ml distilled water and 0.68 g ( $4.3 \times 10^{-3}$  mol) phenylphosphonic acid (Merck). A flat-bottom reaction vessel was connected to a reflux condenser and heated to 70 °C under mechanical agitation for three days. The reacted material was washed and centrifuged 5 times, and the resulting solid was dried at 50 °C for 24 h.

For the powder X-ray diffraction (XRD) analysis, the solid material was placed on a glass sample holder and spread out to form a thin layer. A Rigaku diffractometer using Ni-filtered Co-K<sub>α</sub> radiation ( $\lambda = 1.7902$  Å) with a dwell time of 1° min<sup>-1</sup>, in the  $\theta$ -2 $\theta$  Bragg–Brentano geometry was employed. All measurements were made using a generator voltage of 40 kV and an emission current of 20 mA. Silicon powder was used as the internal standard. In order to remove undesirable fluorescent radiation, a graphite monochromator was used.

Both thermogravimetry (TG) and differential scanning calorimetry (DSC) measurements were carried out simultaneously using Netzsch Model STA409EP Series equipment. The experiments were carried out in static air, using 0.085 cm<sup>3</sup> alumina crucibles. Approximately 15 mg of each sample were analyzed between 20 and 1000 °C with a heating rate of 8 °C min<sup>-1</sup>. The calibration was performed with empty crucibles under the same experimental conditions and the calibration curve was subtracted from the experimental results.

Fourier transform infrared (FTIR) spectroscopy was carried out using a Bomem Michelson MB100 spectrophotometer. Special KBr discs were prepared after mixing (1%) each of the test samples with dry KBr. Grinding of the mixtures was avoided. Analyses were performed in the transmission mode in the 400–4000 cm<sup>-1</sup> range, with a resolution of 2 cm<sup>-1</sup> and accumulation of 16 scans.

The X-ray photoelectron spectra (XPS) were collected using a VG Microtech ESCA3000 system with a base pressure of  $2 \times 10^{-10}$  mbar. No attempt to remove the surface contaminants was undertaken before measurements. The spectra were collected using Mg-K<sub>α</sub> radiation and the overall energy resolution was approximately of 0.8 eV. The energy scale was calibrated using the Si 2p silicate peak at 102.5 eV.<sup>21</sup>

Elemental quantification was carried out on detailed high resolution spectra of the relevant elements using spectral data processing software.<sup>22</sup> The spectra shown in the figures were normalized without background subtraction.

The morphological and electron diffraction study was performed using a JEOL 1200 EX-II transmission electron microscope operating at 60 kV. The crystals were suspended in water with manual stirring, deposited by casting directly on a copper grid (diameter 3 mm) previously covered with a parlodium film and dried at room temperature for several hours.

The energy dispersive X-ray (EDX) measurements were carried out with a LEO Model 440 scanning electron microscope operating at 20 kV. An Oxford 7060 detector with a system resolution of 133 eV was used. O, Mg, Al, Si, Ca and Fe standards were used to quantify the atomic percentages of the elements present in the samples. Four different spots on each sample were quantified and the results were uniform and reproducible.

### 3 Results

X-Ray diffractograms of pristine chrysotile and a sample after reaction with phenylphosphonic acid are shown in Fig. 1. Chrysotile [Fig. 1(a)] shows a basal interplanar spacing of 7.36 Å, in agreement with the literature value.<sup>19</sup> Small impurities of talc were identified in the raw sample (peak denoted with a T in the diffractogram).

After reaction with phenylphosphonic acid, a new phase was generated (C-PPA) with a basal interplanar distance of 15.2 Å, as shown in Fig. 1(b). This interplanar distance is consistent with the grafting of phenylphosphonate groups to the layers of chrysotile and is similar to the values obtained for kaolinite ( $c = 15.02$  Å),<sup>16</sup> kaolinite and halloysite ( $c = 15.4$  Å)<sup>17</sup> and phlogopite ( $c = 15.3$  Å)<sup>18</sup> grafted with phenylphosphonate groups after partial disruption of the layers. Single layers of phenylphosphonate would produce lower interplanar distances: aluminium,  $c = 14.35$ <sup>1</sup> and 14.8 Å;<sup>23</sup> copper,  $c = 14.5$  Å;<sup>24</sup> iron,  $c = 14.45$  Å;<sup>25</sup> magnesium,  $c = 14.3$  Å;<sup>26</sup> manganese and cobalt,  $c = 14.34$  Å.<sup>27</sup>

TG/DSC traces for chrysotile and C-PPA are shown in Fig. 2. For chrysotile [Fig. 2(a)], the initial 3.7% mass loss is associated with the elimination of absorbed/adsorbed water

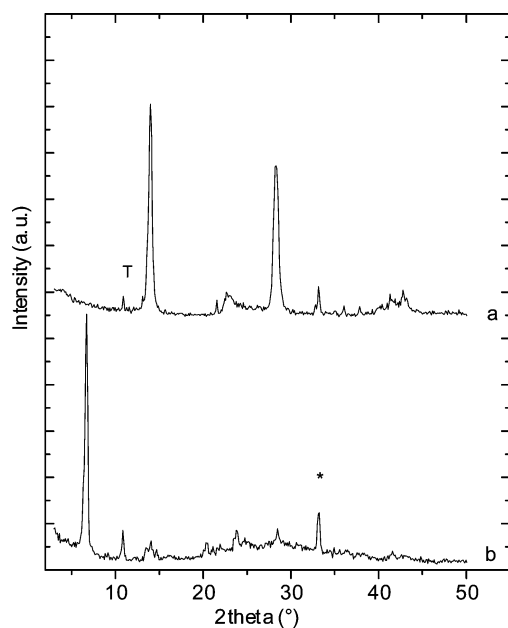


**Fig. 1** X-Ray powder diffractograms of raw chrysotile (a) and of the phenylphosphonate-grafted hybrid (b). Powdered silicon (peak marked with an asterisk) was used as the internal standard.

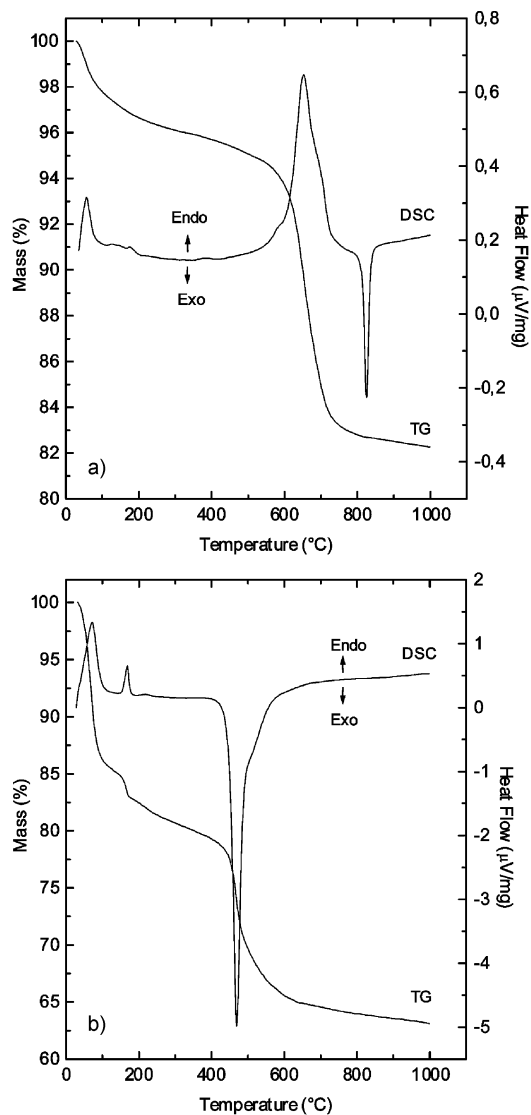


**Fig. 2** TG/DSC traces of raw chrysotile (a) and of the phenylphosphonate-grafted hybrid (b).

molecules (weak endothermic peaks centered at 56, 126 and 173 °C) and is followed by a large endothermic asymmetric peak centered at 653 °C, attributed to the dehydroxylation of the structure. The exothermic peak observed at 825 °C is attributed to the crystallization of  $Mg_2SiO_4$ .<sup>28</sup> The 14.6% mass loss (on the basis of dry matter) due to dehydroxylation is close to the theoretically expected value of 13%. The small deviation can be attributed to the talc impurity in the sample and the presence of substitutional iron and aluminium.

The C-PPA sample [Fig. 2(b)] shows two endothermic peaks at 72 and 169 °C, attributed to water elimination, which amounts to a 18.7% mass loss between RT and 250 °C. The exothermic peak at 469 °C is attributed to the combustion of organic matter. There is an additional mass loss of 22.5% (on the basis of dry matter) between 250 and 1000 °C, attributed to the decomposition of phenylphosphonate and talc impurities {the mass loss step on the basis of wet matter is 18.3% [shown in Fig. 2(b)]}. The thermal behavior is very similar to that of phlogopite, reported earlier.<sup>18</sup> A quantitative determination of the formula is not possible due to the presence of impurities and the unknown composition of the residue after the analysis.

FTIR spectra of chrysotile, brucite and C-PPA are shown in Fig. 3. The spectrum of chrysotile [Fig. 3(a)] displays the typical inner surface Mg–OH stretch ( $3686\text{ cm}^{-1}$ ) and inner Mg–OH stretch ( $3644\text{ cm}^{-1}$ ) absorbances, and broad bands at  $3446$  and  $1630\text{ cm}^{-1}$  attributed to adsorbed/absorbed water

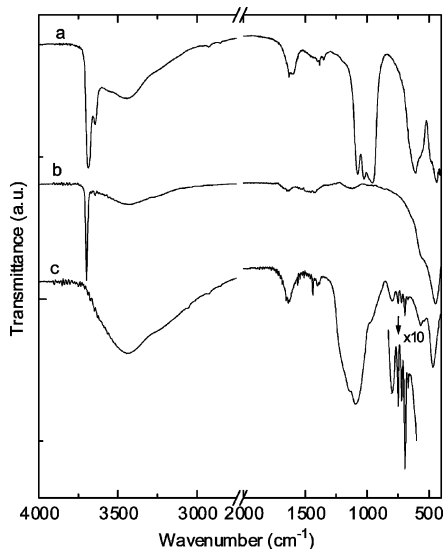


Fig. 3 FTIR spectra of raw chrysotile (a), synthetic brucite (b) and of the phenylphosphonate-grafted hybrid (c).

molecules.<sup>29</sup> The bands at 1077, 1025 and 959  $\text{cm}^{-1}$  can be collectively attributed to Si–O–Si, Si–O–Mg and Si–O stretching vibrations, respectively.<sup>30</sup> The band at 610  $\text{cm}^{-1}$  arises from inner Mg–O vibrations, that at 484  $\text{cm}^{-1}$  from Mg–O vibrations and that at 439  $\text{cm}^{-1}$  to Mg–OH translation or Si–O bending.<sup>31</sup>

The spectrum of brucite displays the typical hydroxyl stretch absorbances at 3698 and 3643  $\text{cm}^{-1}$  and an extended band centered at 3428  $\text{cm}^{-1}$ . We note a small shoulder at 3275  $\text{cm}^{-1}$ , which corresponds to strongly bonded water.<sup>31</sup> Low frequency bands occur at 558 and 447  $\text{cm}^{-1}$ .

The spectrum of the C-PPA sample shows a broad band at 3442  $\text{cm}^{-1}$ , and the absence of Mg–OH absorbances and Mg-related characteristic bands is notable. The appearance of new bands at 695 (phenyl ring), 723, 749 (phenyl ring), 797, 1400 and 1438  $\text{cm}^{-1}$  (P–C stretch)<sup>17</sup> signify that reaction of the organic acid with the mineral has taken place. The Si–O stretch bands are overlapped by a broad collective band with maxima at 1086 (P=O) and 1137  $\text{cm}^{-1}$  (P–O stretching).<sup>17,32</sup>

The frequencies of these latter bands are similar to those observed in the spectra of kaolinite (693, 725, 748, 793 and 1438  $\text{cm}^{-1}$ ),<sup>16</sup> phlogopite (693, 724, 748 and 1438  $\text{cm}^{-1}$ )<sup>18</sup> and kaolinite/halloysite (693, 749, 1164, 1207 and 1439  $\text{cm}^{-1}$ ) grafted with phenylphosphonic acid.<sup>17</sup>

Fig. 4 shows XPS surveys of chrysotile and C-PPA. The spectrum of chrysotile shows the characteristic peaks of Mg, Al, Si, C and O. Quantification in at% of the elements at the

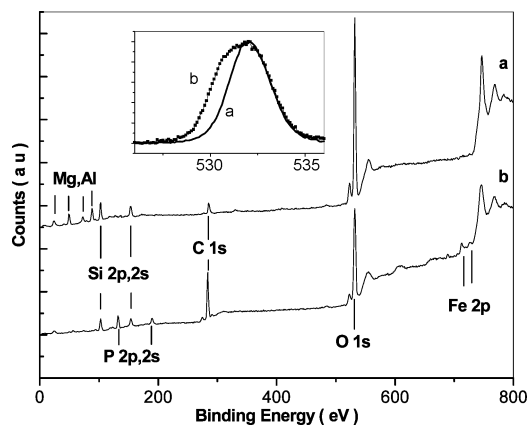


Fig. 4 XPS surveys of raw chrysotile (a) and of the phenylphosphonate-grafted hybrid (b). The inset shows the characteristic O 1s peaks of chrysotile (a) and of the hybrid, C-PPA (b).

surface gives the following composition: Mg 27.5%, Al 6.8%, Si 13.6%, C 7.0% and O 45%. The different quantification of these elements as compared to the chemical and EDX results clearly reflects the peculiar fiber structure, where the octahedral Mg and Al sheet hides the inner silicate tetrahedral sheet. The carbon peak is attributed to adventitious carbon on the mineral, which was exposed to air.

The spectrum of the grafted sample, on the other hand, shows dramatically reduced magnesium and aluminium peaks. Note the presence of phosphorus and the increased amount of carbon in the reacted sample. Peaks due to the iron impurities are also visible. Quantification in at% of the elements at the surface gives the following composition: Mg 1.6%, Al 1.7%, Si 11.6%, P 9.0%, C 38.0%, O 36.4% and Fe 1.6%. This result shows the almost complete leaching of Mg and Al and the incorporation of P and C from the phenylphosphonate groups. The inset of Fig. 4 shows the characteristic O 1s peaks of chrysotile and of the hybrid. The peak of the grafted sample unambiguously shows the presence of a new component at a lower binding energy. This component is associated with oxygen within the phenylphosphonate groups.

The EDX measurements yielded the following composition (at%) for chrysotile: O 57.3%, Mg 22.4%, Al 0.6%, Si 18.5%, Ca 0.2% and Fe 0.9%. These EDX results are in good agreement with the chemical analysis,<sup>20</sup> which gave the following composition (wt%): SiO<sub>2</sub> 42.5% (19.9% Si), Al<sub>2</sub>O<sub>3</sub> 1.12% (0.6% Al), MgO 38.2% (23% Mg), Fe<sub>2</sub>O<sub>3</sub> 4.05% (2.8% Fe) and H<sub>2</sub>O 14.13%.

The EDX data for the grafted C-PPA sample, in contrast, show that complete modification of the elemental composition (at%) compared to the starting material: O 52.9%, Mg 0.2%, Al 1.3%, Si 35.9%, P 7.2% and Fe 2.6%. Excluding interference from the impurities, the average Si/P ratio is 5.5 Si/P in C-PPA.

Fig. 5(a) shows a bright-field image of the characteristic chrysotile fibers. The maximum and minimum outer radii of the fibers are around 281 and 179 Å, respectively. The inset shows a close-up of a fiber with an inner radius of about 124 Å and an outer radius of about 179 Å. The cylindrical sheets are concentrically closed. Apparently, all rolled forms present a uniform material inside.

Fig. 5(b) shows a bright-field image of the new material,

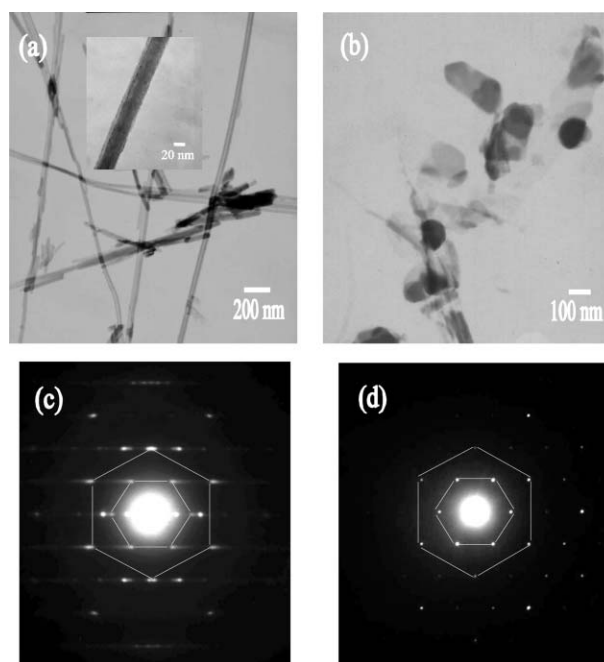


Fig. 5 Typical morphology of chrysotile fibers (a) and of the phenylphosphonate-grafted hybrid (b). The corresponding selected area electron diffraction patterns are shown in (c) and (d), respectively. The inset in (a) shows a close-up of a single chrysotile fiber.

which consists of stable layered structures with some residual chrysotile fibers. Fig. 5(c) shows the SAED pattern of the chrysotile fibers, with a typical diffraction pattern consisting of diffraction spots lying along parallel lines (so-called layer lines), whose separation gives the crystallographic parameter  $a$  parallel to the fiber axis. In this case, the  $a$  parameter is found to be 5.80 Å. Fig. 5(d) shows the SAED pattern of the new stable reacted hybrid material with a clear hexagonal structure, consisting of a basal lattice parameter  $a' = 5.62$  Å. It is remarkable that this hexagonal structure corresponds to a sub-structure of the fiber diffraction pattern of chrysotile, i.e. the same hexagonal structure with  $a' = 5.62$  Å appears superimposed on the layer lines (see hexagonal diagrams) in the SAED pattern of chrysotile.

Since chrysotile fibers consist of a cylindrical arrangement of rolls with stacking of the octahedral and tetrahedral sheets in a pseudo-hexagonal planar structure, the pre-existing tetrahedral and octahedral sheets are the natural candidates to form the structural unit of the new material obtained by the leaching/grafting reaction, with some degree of distortion, as is clearly shown in the SAED patterns. Therefore, it is most probable that the new stable layers are formed from the silica tetrahedral sheets, since all the characterization data clearly show leaching of the brucite sheets.

#### 4 Discussion and conclusions

The reaction of chrysotile fibers with phenylphosphonic acid in distilled water led to a new layered material. From the structural point of view, both powder XRD and TEM confirm the evolution of the chrysotile rolled fibers into small planar lamellae. Added to this, powder XRD also evidences the clear expansion of the basal interplanar distance, indicating the insertion of new groups into the original mineral. XPS and EDX analyses show unambiguously that magnesium is removed from the original silicate and that phenylphosphonate groups are present in the new hybrid. Thermal TG and DSC as well as FTIR measurements confirm the grafting of those groups to the silicate.

This new hybrid nanocompound is essentially formed from planar silica sheets, as is clearly shown by the SAED results. We think that the phenylphosphonate groups are grafted to newly generated silane groups on both sides of the silica layers, although grafting to one side plus the contribution of water molecules also leads to the same interplanar basal distance.

The chemical removal of the octahedral magnesium structure first causes unrolling of the fibers, accompanied by some rupturing, leading to the small layered plaques seen in the TEM images, and, secondly, the grafting of phenylphosphonate groups to the bare lamellae. Thus, treatment of chrysotile with phenylphosphonic acid promotes the leaching of the brucite octahedral sheet bonded to the trydimite tetrahedral sheet with concomitant anchoring of the phenylphosphonic groups.

Chrysotile has structural layers consisting of pseudo-hexagonal sheets of bonded silica tetrahedra with lattice parameters  $a = 5.3$  Å and  $b = 9.2$  Å. All the tetrahedra inside the sheet have the same spatial orientation and are bonded to the brucite layer, where there are two types of oxygen: bridging (shared by two tetrahedra) and apical (bonded to one tetrahedron). Hence, the apical oxygen needs to be bonded after leaching. The apical oxygen represents the most favorable site to start the grafting reaction with phenylphosphonate groups after brucite layer disruption. Finally, it is worth noting that the lattice parameter of the new material is not far from the value of the crystallographic parameter parallel to the fiber axis of chrysotile. The hexagonal diagram in the SAED pattern of the new hybrid material shows a small expansion (1.1%) along the layer lines compared to the hexagonal diagram in the SAED pattern of chrysotile. Another

synthesis conducted in toluene produced a compound with an identical interplanar basal spacing.

#### Acknowledgements

The authors gratefully acknowledge the Fundação Araucária and CNPq for financial support, the X-Ray Optics Group, Departamento de Física da UFPR, for access to the X-ray diffractometer, the Centro de Microscopia Eletrônica da UFPR for use of the transmission electron microscope and SAMA—Mineração de Amianto Ltda, for the supply of chrysotile samples.

#### References

- 1 F. Wypych, W. H. Schreiner and R. Marangoni, *J. Colloid Interface Sci.*, 2002, **253**, 180–184.
- 2 J. L. Guimarães, R. Marangoni, L. P. Ramos and F. Wypych, *J. Colloid Interface Sci.*, 2000, **227**, 445–451.
- 3 L. Raki and C. Detellier, *Chem. Commun.*, 1996, 2475–2476.
- 4 C. Hornick, P. Rabu and M. Drillon, *Polyhedron*, 2000, **19**, 259–266.
- 5 S. Ogata, H. Tagaya, M. Karasu and J. Kadokawa, *J. Mater. Chem.*, 2000, **10**, 321–327.
- 6 M. Inoue, Y. Kondo and T. Inui, *Inorg. Chem.*, 1988, **27**, 215–221.
- 7 M. Inoue, H. Tanino, Y. Kondo and T. Inui, *Clays Clay Miner.*, 1991, **39**, 151–157.
- 8 M. Inoue, H. Kominami, Y. Kondo and T. Inui, *Chem. Mater.*, 1991, **9**, 1614–1619.
- 9 M. G. Fonseca and C. Airoidi, *Mater. Res. Bull.*, 2001, **36**, 277–287.
- 10 J. Tunney and C. Detellier, *J. Mater. Chem.*, 1996, **6**, 1679–1685.
- 11 J. Tunney and C. Detellier, *Chem. Mater.*, 1993, **5**, 747–748.
- 12 J. Tunney and C. Detellier, *Clays Clay Miner.*, 1994, **42**, 552–560.
- 13 J. Tunney and C. Detellier, *Clays Clay Miner.*, 1994, **42**, 473–476.
- 14 Y. Komori, H. Enoto, R. Takenawa, S. Hayashi, Y. Sugahara and K. Kuroda, *Langmuir*, 2000, **16**, 5506–5508.
- 15 Q. Liu, D. A. Spears and Q. Liu, *Appl. Clay Sci.*, 2001, **19**, 89–94.
- 16 J. L. Guimarães, P. Peralta-Zamora and F. Wypych, *J. Colloid Interface Sci.*, 1998, **206**, 281–287.
- 17 C. Breen, N. D'Mello and J. Yarwood, *J. Mater. Chem.*, 2002, **12**, 273–278.
- 18 C. Trobajo, S. A. Khainakov, A. Espina, J. R. Garcia, M. A. Salvado, P. Pertierra, S. Garcia-Granda, A. Martin-Izard and A. I. Bortun, *Chem. Mater.*, 2001, **13**, 4457–4462.
- 19 G. W. Brindley and G. Brown, *Crystal Structure of Clay Minerals and their X-Ray Identification*, Mineralogical Society, London, 1980.
- 20 M. G. Fonseca, J. A. Simoni and C. Airoidi, *J. Colloid Interface Sci.*, 2001, **240**, 533–538.
- 21 J. F. Moulder, W. F. Sobol and K. D. Bomben, *Handbook of X-ray Photoelectron Spectroscopy*, Physical Electronics Inc., Eden Prairie, 1995.
- 22 Spectral Data Processor, Version 3.2, XPS International, Mountain View, CA, USA, 2001.
- 23 J. E. Haky, J. B. Brady, N. Dando and D. Weaver, *Mater. Res. Bull.*, 1997, **32**, 297–303.
- 24 G. B. Hix, V. C. Maddocks and K. D. M. Harris, *Polyhedron*, 2000, **19**, 765–770.
- 25 C. Bellitto, F. Federici, A. Altomare, R. Rizzi and S. A. Ibrahim, *Inorg. Chem.*, 2000, **39**, 1803–1808.
- 26 G. Cao, L. Lee, V. M. Lynch and T. E. Mallouk, *Inorg. Chem.*, 1988, **27**, 2781–2785.
- 27 J. T. Culp, G. E. Fanucci, B. C. Watson, A. N. Morgan, R. Backow, H. Ohnuki, M. W. Weisel and D. R. Talham, *J. Solid State Chem.*, 2001, **159**, 362–370.
- 28 J. Khorami, D. Choquette, F. M. Kimmerle and P. K. Gallagher, *Thermochim. Acta*, 1984, **76**, 87–96.
- 29 E. Mendelovici, R. L. Frost and J. T. Kloprogge, *J. Colloid Interface Sci.*, 2001, **238**, 273–278.
- 30 T. Sugama, R. Sabatini and L. Petrakis, *Ind. Eng. Chem. Res.*, 1998, **37**, 79–88.
- 31 R. L. Frost and J. T. Kloprogge, *Spectrochim. Acta, Part A*, 1999, **55**, 2195–2205.
- 32 C. T. Seip, G. E. Granroth, M. W. Meisel and D. R. Talham, *J. Am. Chem. Soc.*, 1997, **119**, 7084–7094.